Liquid Metal Actuators: Correctable Mounting and Assembly of Thin-Shell X-ray Telescope Mirrors

Alexander R. Bruccoleri[a], Martin Klingensmith[b], Brandon Chalifoux[b], Ralf K. Heilmann[b] and Mark L. Schattenburg[b]

[a]Izentis LLC, 303 3rd St. # 101, Cambridge, MA 02142, USA
[b]Space Nanotechnology Laboratory, MIT Kavli Institute for Astrophysics and Space Research, Massachusetts Institute of Technology, Cambridge, MA 02139, USA

ABSTRACT

An ideal bonding agent for thin-shell x-ray mirrors could be quickly applied to joints and set with deterministic and stable properties. Unfortunately, mirror assembly methods have typically utilized various epoxy formulations which are messy, slow to apply and cure, and far from deterministic or stable. Problems include shrinkage, creep and high thermal and humidity sensitivity. Once the bond is set errors are frozen in and cannot be corrected. We are developing a new method for bonding thin-foil mirrors that has the potential to solve these problems. Our process to bond mirrors to housing reference points is achieved via small beads of a low-melting-point bonding agent (such as solder or thermoset). The mirror is bonded to small contact surface points under real-time metrology. If the position of the mirror needs to be adjusted after bonding, a small force is applied normal or parallel to the contact surface and a pulsed fiber laser is used to melt an ultrathin layer of the solder for a very short time. The joint is then compressed, stretched or sheared while molten before refreezing in a new position, enabling repeatable and stable mirror position adjustments along the direction of the force in nm-level steps with minimal heat input. We present results from our prototype apparatus demonstrating proof of principle. The initial experiment includes developing a technique to bond D263 glass to Kovar, designing and building a one-dimensional stage to precisely apply force, and using an infrared laser pulse to heat the joint while measuring position and force.

Keywords: Precision Engineering, Solder, Adjustable Bonding, Liquid Metal, Laser Heating, X-ray Optics

1. INTRODUCTION

This paper presents a new technique to bond transparent objects to metal that enables precise nanometer adjustment after bonding. The concept is to form the initial bond via solder and then to heat the joint with a brief laser pulse while applying a force to move it. The laser pulse is carefully designed to melt the surface of the solder allowing for movement while not adding enough energy to vaporize or damage the joint. This technique is termed "liquid metal actuation" and can be applied to any project where transparent objects need to be bonded to a frame with nanometer precision. The specific application for this development is the bonding of thin-shell x-ray telescope mirrors. Astronomy x-ray telescopes are at a high level of technical maturity as reviewed by O'Dell et al.;[1] however, there is desire for telescopes with collecting areas $\sim$1 m^2 with sub 1 arc-second angular resolution such as the X-ray Surveyor mission concept.[2] Science objectives and x-ray telescope concepts are further described in the New Worlds New Horizons Decadal Review[3] and in the Enduring Quests Daring Visions Astrophysics Roadmap[4] and references therein.

One of the most viable mirror technologies under development for large collecting area and high resolution is the segmented approach by Zhang et al.[5] at NASA Goddard Space Flight Center (GSFC). The concept is to thermally shape $\sim$200 mm rectangular glass sheets into parabolic and hyperbolic Wolter mirror shapes, and then carefully assemble the mirrors into a frame to create a large collecting area optic. The advantage of this technique is that small mirrors can be assembled together and scaled to much larger mirror area. At present this technique has demonstrated 8.3 arc-second resolution with an assembly of three mirror pairs.[5] The largest

Further author information: (Send correspondence to Dr. Alexander Bruccoleri)
E-mail: alex@izentis.com

source of error is the mirror figure composed of slumping and mandrel figure errors, followed by errors caused by coating stress, alignment, metrology, and bonding.[5,6] GSFC is investigating technologies to reduce the mirror error such as polished thin silicon mirrors,[5] and MIT is developing porous air bearing mandrels along with a novel ion implant technique,[8] all of which are aimed at reducing these mirror figure errors. Furthermore NASA Goddard and Marshall Space Flight Centers and collaborators are making progress on coating stress, alignment and metrology.[5–7,9] At present there is little effort put into improving the bonding process and that is where liquid metal actuation could improve resolution. The current state-of-the-art for bonding x-ray telescope mirrors to an external frame utilizes epoxy which is unstable, nondeterministic and slow to apply and cure. The bonding process developed by Zhang et al.[5,6,9] at GSFC is as follows: six L-shaped, glass-to-metal, expansion-matched metal clips are bonded to the mirror via epoxy. 2 and 1 for computer aided drawings and photographs of the GSFC bonding technique.

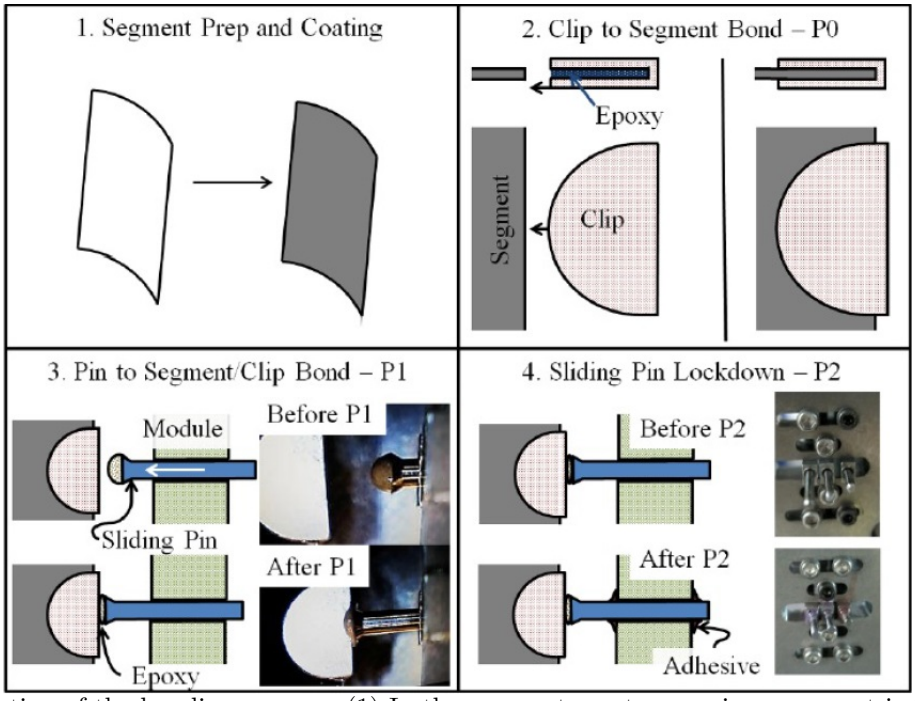

Figure 1: Illustration of the bonding process. (1) In the preparatory step, a mirror segment is fabricated and a metallic film is deposited and annealed. (2) Clips are attached to the mirror to spread the load and enlarge the area for subsequent bonding. Three clips are attached on each side of a mirror. Note that in the latest version, only half-clips, are used which are attached to the mirror only at its backside. (3) After the mirror is properly aligned, six sliding pins with epoxy contact the clips and the epoxy is left to cure over the next day. (4) In the final step, the sliding pins are locked down with cyanoacrylate adhesive in their bushings which are a structural part of the module. The complete process is performed in a stable thermal environment. (Figure and caption from Chan et al.[9])

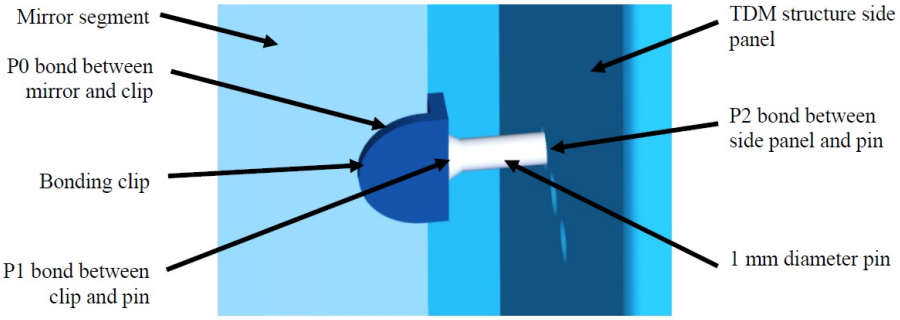

Figure 2: Detail of structural connection between mirror segments and technology development module (TDM) structure including P0, P1 and P2 bonds. (Figure and caption from McClelland et al.[6])

The epoxy shrinks during curing so the epoxy is cured slowly in an oven for up to five days to minimize shrinkage. A hexapod and a precise metrology tool are used to hold the mirror in the housing frame. Metallic pins are then bonded to the clips via epoxy, so that the pins can slide freely in shafts as the epoxy cures. After curing, the pins are bonded to the metal frame with cyanoacrylate glue. This technique is slow as each mirror takes at a least a full day to bond. See Figures

Epoxy joints yield unpredictable results, which are acceptable for a 5 arc-second telescope but not for sub arc-second resolution.[9] Furthermore, epoxy is undesirable due to high shrinkage, large coefficient of thermal expansion (CTE) and creep, resin aging effects, water absorption, outgassing, low tensile strength, exothermicity, and requiring large amounts of time and/or heat to cure. Solder joints represent an advantage over epoxy since they can be adjusted after the bond, and the bonds can be done in under an hour. Sapphire rods could replace the metal rods, and they could be soldered instead of epoxied onto the L-shaped clips on the mirrors. Sapphire is strong and transparent to infrared (IR), which allows for a laser to heat the joint. Ideally the heat would melt a small region of the solder and the joint could be compressed, stretched or sheared by a desired amount. The adjustment needs to be small enough to allow for sub arc-second angular resolution. For example a $\sim$100 nm adjustment leads to an angular adjustment resolution of $<$1 μrad or 0.2" for a 200 mm-wide segmented x-ray telescope mirror, which is a reasonable experimental goal. See Figure 3 for a drawing of the alignment goal and Figure 4 for drawings of the solder joint concept. To evaluate the feasibility of this technique, an experiment was conducted with Kovar rods soldered to D263 glass.

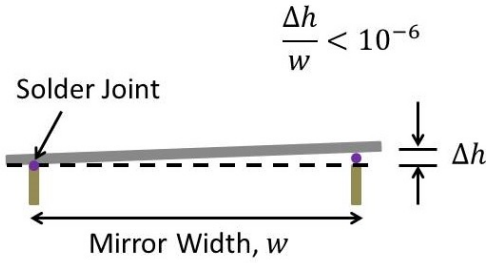

Figure 3: Drawing of gap-thickness adjustment goal for liquid metal actuation.

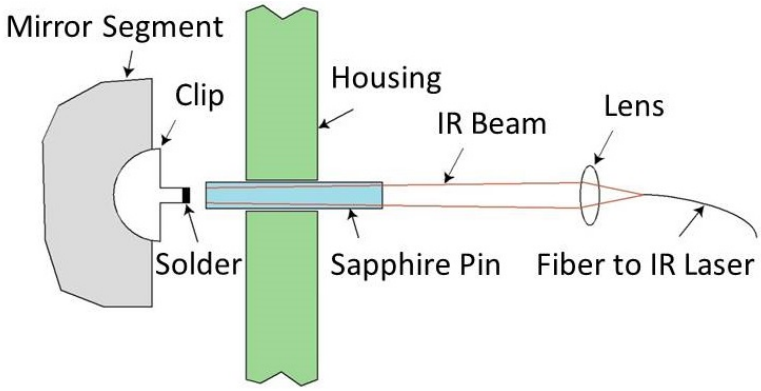

(a) The process is similar to the current GSFC technique, except that a glass or sapphire pin is used instead of stainless steel and the clip is equipped with a solder pad. Heat is delivered to the bond via an external fiber IR laser.

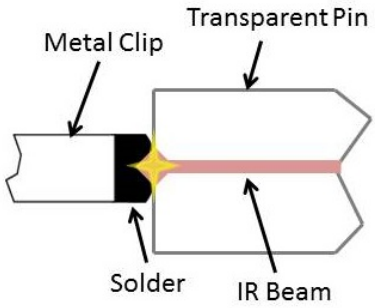

(b) Detail of region near the clip and pin surfaces. The solder is machined into a slight dome to ensure deterministic contact as the pin is pushed to touch the cold solder. IR radiation is then applied to heat the surface of the solder pad.

Figure 4: Illustration of proposed pin bonding process.

2. THEORY OF BOND ACTUATION

The physical concept behind liquid metal actuation of solder bonds is to momentarily heat and liquify a thin layer of the bond while applying a force to compress, stretch or shear it. This requires applying a precise amount of heat which can be achieved with an infrared (IR) laser. The laser intensity must not be too low, to avoid excessive heat from diffusing through the entire joint with a peak temperature below the melting point. Alternatively, too much intensity will vaporize a thin layer and destroy the joint. This problem can be thought of as adding heat to one end of an infinite rod. It can be solved analytically, starting with the one-dimensional heat equation;

$$\lambda \frac{\partial^2 T}{\partial x^2} + \dot{Q} = \rho c_p \frac{\partial T}{\partial t}, \tag{1}$$

where λ is the thermal conductivity, T is the temperature, t is time, x is the spatial dimension, $\dot{Q}$ is the power absorbed per unit volume, ρ is the density and c_p is the specific heat at constant pressure. See Figure 5 for a depiction of the heat flow in the solder.

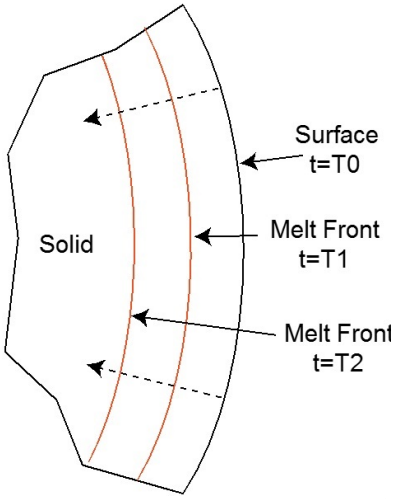

Figure 5: Depiction of the melt front propagating into the solder pad. At beam turn-on time T0 the surface of the cold solder is solid. A melt front propagates as shown at times T1 and T2.

A solution was presented by Zhuang et al.,[10]

$$T(x,t) = T_{A0} + \frac{\dot{q}_0}{\lambda}\sqrt{\frac{4kt}{\pi}}\left[exp\left(-\frac{x^2}{4kt}\right) - x\sqrt{\frac{\pi}{4kt}erfc\left(\frac{x}{\sqrt{4kt}}\right)}\right], \tag{2}$$

where T_{A0} is the initial surface temperature, $\dot{q}_0$ is the heat transfer, k is the thermal diffusivity defined as $\lambda/\rho c_p$ and $erfc$ is the complementary error function defined as;

$$erfc(z) = \frac{2}{\sqrt{\pi}}\int_z^\infty \mathrm{e}^{-t^2}\,\mathrm{d}t. \tag{3}$$

This solution can be graphed for various heat fluxes and materials to estimate the temperature profile in the rod at given times. The desired thickness of the molten region was not precisely known for the experiments presented, and ~10 μm was chosen as a starting thickness. For 60/40 lead/tin (Pb/Sn) solder, the temperature profile after a 1 milli-second pulse with 50 Watts being absorbed at the surface over a 1 mm^2 area is plotted in Figure 6. This ignores the latent heat of fusion of solder and assumes constant material properties over the temperature range.

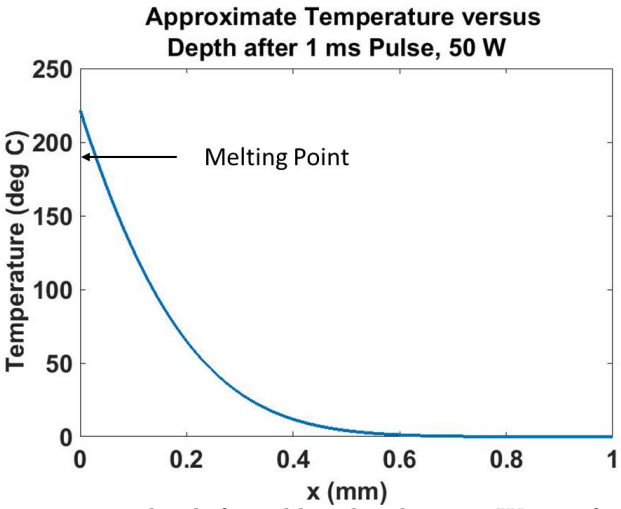

Figure 6: Predicted temperature versus depth for solder absorbing 50 Watts of energy at one end for a 60/40 Pb/Sn solder joint. The first few tens of microns are heated above 183 C, the melting point of the solder.

This modeling suggests it is possible to momentarily melt a ∼10 μm layer of solder. Laser pulses of this intensity and duration are easily achieved with IR fiber lasers used in the cutting and welding industry.

3. EXPERIMENTAL APPARATUS

A simple test bench was built to test the concept of liquid metal actuation. There are six degrees of freedom in the solder joint and the experiment tested one of them, movement normal to the glass surface. The other five degrees of freedom include two shear, which is motion parallel to the surface, and three for rotations. Kovar pins were soldered to D263 glass, and an IR laser irradiated the joint from the glass side while a normal force was applied. The apparatus consisted of a steel base with a one-dimensional stage driven with a micrometer. The micrometer pushes against a bracket with a load cell mounted to it. A hexagonal steel bar with slots for the Kovar pin and two capacitance gauges was mounted to the load cell. The size change of the solder joint in the normal direction to the glass was monitored via capacitance gauges. The capacitance gauges were securely mounted with the Kovar pin in the steel bar, and they measured the gap-thickness change between the glass and their front surfaces. Two aluminum blocks were used to the hold the D263 glass in place. One block was bolted to the steel base. The D263 glass was epoxied onto the other aluminum block, which was bolted to the main aluminum block. The advantage of using two blocks is the main block can be aligned on the steel base, and the second block can then be replaced with new samples without requiring realignment. This allowed for quick sample replacement, which was important as this experiment was done at a remote facility with limited time. See Figure 7 for a conceptual drawing of the apparatus.

The procedure to solder the D263 glass to the Kovar pin is as follows: The glass was piranha cleaned (3:1 mixture of 96% H_2SO_4 and 30% H_2O_2 respectively by weight) and then 5 nm of chrome followed by 10 nm of gold was evaporated onto the glass. 60/40 Pb/Sn solder does not adhere to glass surfaces; however, it does adhere well to gold. Chrome was used as an adhesion promoter between gold and glass. The bi-layer of chrome and gold had to be thin (∼ 10 nm) to prevent absorption of the IR laser beam. The Kovar and post-evaporated glass were cleaned via acetone and isopropyl alcohol. A small (∼1 mm) bead of solder was wicked onto the tip of the Kovar with a soldering iron set to 660° F. The rod was held vertically with an aluminum jig which allowed the rod to rest vertically against the glass. The glass and the rod were placed on a hot plate set to 400° C, and were removed when the solder melted. After cooling the bonded pieces were removed from the jig. This technique yielded very strong bonds. No formal mechanical strength testing was done; however, the glass would break or delaminate before the bonds would break during testing. It should be noted that the soldering technique used via hot plate was intended for the experiment of liquid metal actuation. This technique could distort a telescope mirror, and local heating via laser would be used instead for a precision optic.[11] See Figure 8 for a picture of a D263 sample bonded to a Kovar pin.

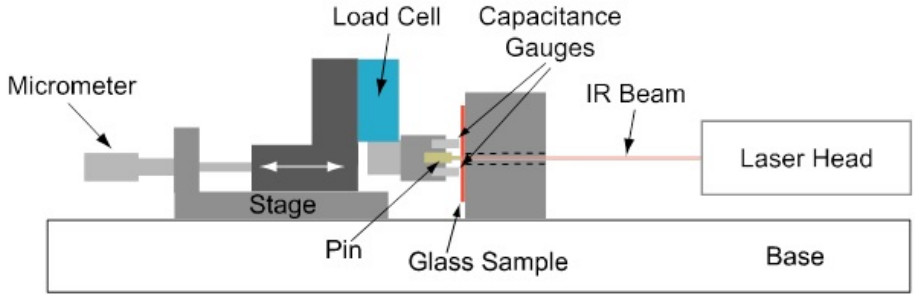

Figure 7: Conceptual drawing of solder actuator test stand. A Kovar pin is soldered to a glass sample and then the pair is loaded into the test stand. First the Kovar pin is clamped into the movable hexagonal pin block and then the sample is bonded to a stationary sample block. A micrometer applies force to push or pull the pin, with force measured by a load cell. Gap-thickness changes of the solder joint between laser pulses is measured with a pair of capacitance gauges. The cap gauges were arranged in a horizontal plane in the pin block, but for clarity are shown in a vertical plane.

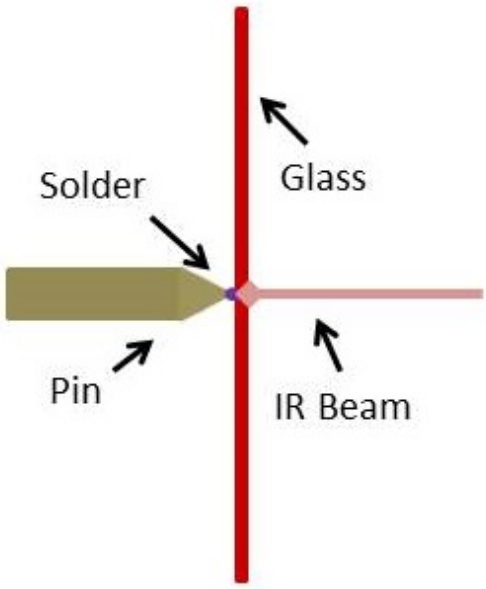

(a) Conceptual drawing of pin attached to glass with laser irradiation.

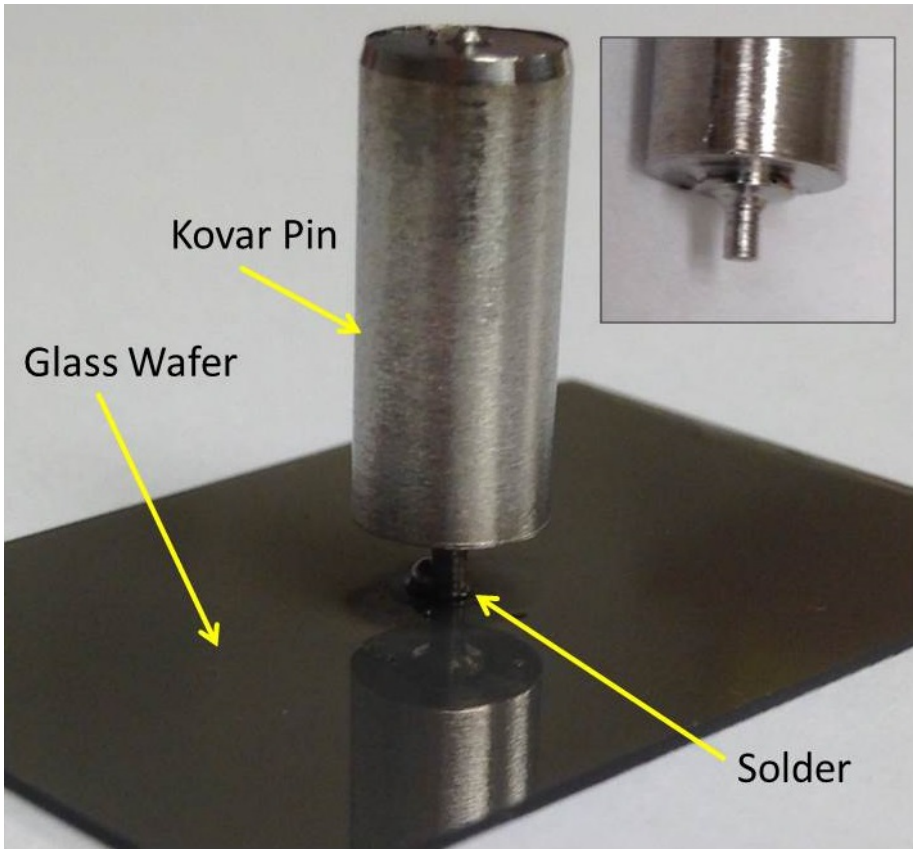

(b) Photograph of Kovar pin soldered to a D263 glass wafer chip (∼1 cm x ∼2 cm). The wafer is coated with a thin chrome and gold layer to promote solder adhesion. Surface discoloration and blob of solder to left of pin are due to hand soldering.

Figure 8: Photograph and drawing of the experiment.

The apparatus was mounted to a micrometer stage and placed inside a large metal housing at the Applications Lab at IPG Photonics Inc. The laser to irradiate the joint was a quasi-CW 450 W ytterbium fiber laser Model YLS-450-4500 QCW, with an emission wavelength of 1070 nm. The laser was aligned by IPG Photonics Inc. and irradiated the sample from the back as depicted in Figure 7. Once the sample was mounted, force between $\pm \sim$10 N was applied and the gap-thickness change was monitored with the capacitance gauges. After the gap thickness stabilized, a laser pulse was initiated and the gap thickness was measured. The joint would initially expand, which was attributed to thermal expansion, and then contract to a steady state value which was considered the post-pulse gap thickness.

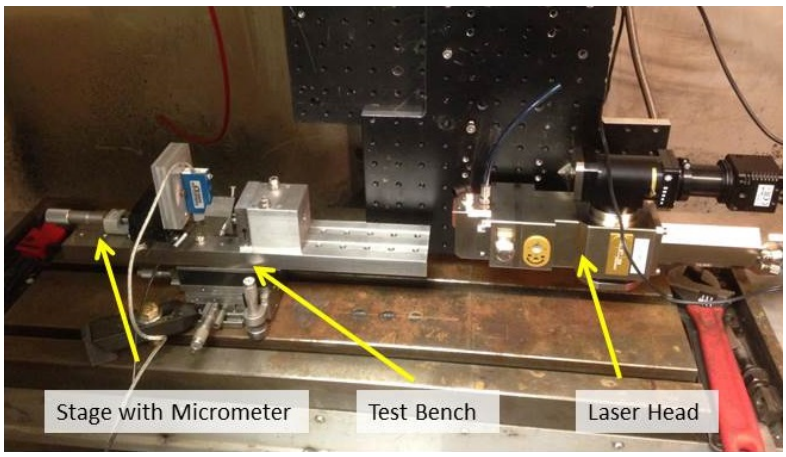

(a) Test bench and laser head in a 3-axis stage at IPG Photonics laboratory.

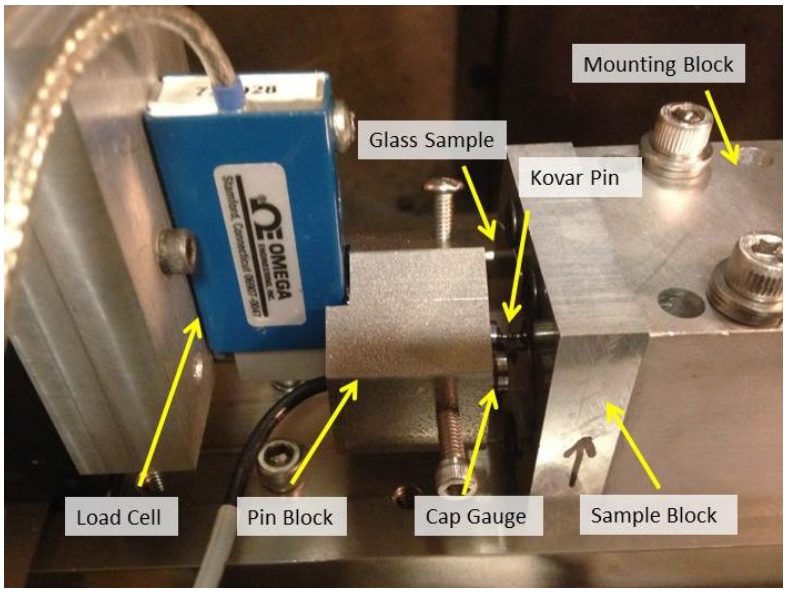

(b) Detail of test bench showing sample with soldered pin. The pin base is clamped into the pin block and the glass sample is bonded to the sample block. The sample and pin can be pushed or pulled apart using a small precision stage with micrometer head. A load cell measures force while a pair of capacitance gauges measure gap-thickness change.

Figure 9: Bond actuator test setup.

Glass deflection was considered as a possible source of error. The glass is epoxied over a hole for the laser to irradiate the glass and it is possible that the glass could deflect. Changes in the force applied could then result in a change in the gap thickness. The epoxy was carefully applied such that the hole open diameter was ∼1 mm, which is roughly the same size as the joint. This approximates a circular glass plate, with a uniform load and the edges clamped. The approximate solution for the maximum deflection is derived by Beardmore;[12]

$$y_m = \frac{0.179pr^4}{Et^3}, \tag{4}$$

where y_m is the maximum deflection, p is the uniform load, r is the radius of the hole, E is Young's modulus of elasticity and t is the thickness of the glass. Poisson's ratio is assumed to be 0.208 and Young's modulus of elasticity is assumed to be 72.9 GPa.[13] For a 0.5 mm-thick piece of glass with 1 Newton distributed over 1 mm^2, the maximum deflection is plotted in Figure 10. A 1 mm-diameter hole gives a deflection of ≈ 1 nm with 1 Newton of force, which is negligible.

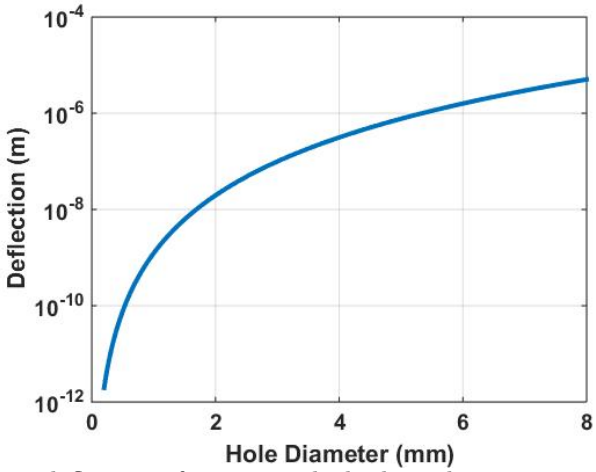

Figure 10: Maximum deflection of 0.50 mm-thick glass plate, 1 newton of force over 1 mm^2.

4. EXPERIMENTAL RESULTS

The experimental data is summarized in Figure 11. The results show an increase in gap thickness under tensile force and a decrease with compressive force. Low or zero force resulted in no measurable motion and the noise floor in these measurements is approximately 20 nm. The amount of change is strongly correlated with the pulse energy (pulse length x power), which should lead to a thicker melted layer, and thus less resistance to flow. Gap-thickness changes per laser shot ranged from ≈ 50 to 400 nm which is a promising result. Figure 12 summarizes this result by plotting average gap-thickness change vs. pulse energy. The designations "S1" and "S2" in Figure 11 refers to samples 1 and 2, respectively. Both samples were soldered by hand and the joint was roughly 2 mm^2 for sample 1 and 4 mm^2 for sample 2. As a result it took more laser energy and force for sample 2 than sample 1 to see a change.

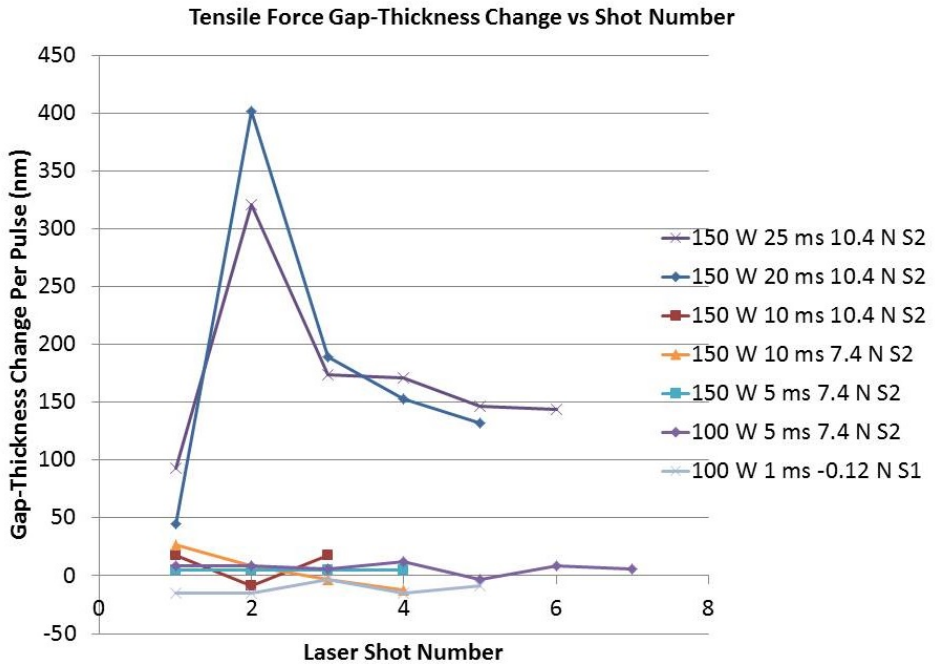

(a) Measured gap-thickness change per shot vs. laser shot number for two samples (S1 and S2), and a range of laser powers (100-150 W), pulse times (1-25 ms), and tensile and $\sim$ neutral forces (-0.12 to 10.4 N).

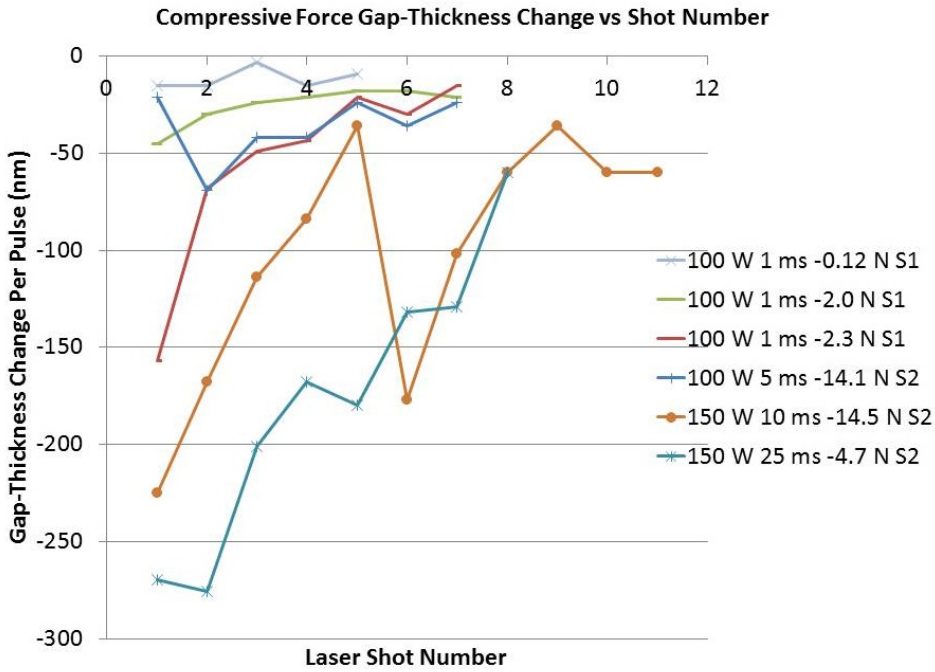

(b) Measured gap-thickness change per shot vs. laser shot number for two samples (S1 and S2), and a range of laser powers (100-150 W), pulse times (1-25 ms), $\sim$ neutral and compressive forces (-14.5 to -0.12 N).

Figure 11: Results of tests at IPG Photonics lab.

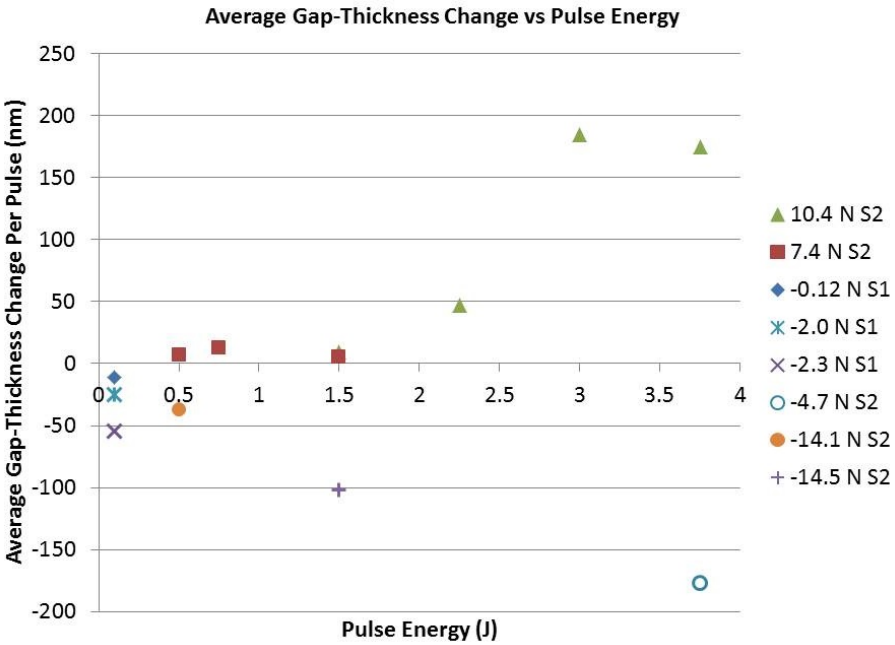

Figure 12: Average gap-thickness change from Fig. 6a vs. pulse energy. Tensile force (> 0 N) results in positive change, while compressive force (< 0 N) results in negative change. Higher pulse energies result in larger changes.

5. ANALYSIS

The results show a promising result; the gap thickness can be changed < 100 nm by applying a force while irradiating the joint with an IR laser. The physics behind this process is complicated and precisely modeling this technique is challenging. It can be modeled as a thin fluid between two parallel plates with a normal force applied that squeezes out the fluid tangent to the surface as depicted in Figure 13.

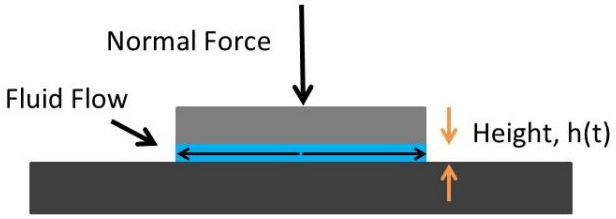

Figure 13: Depiction of a fluid between two plates. The gap thickness is defined as h(t).

The approximate relationship between the rate of change for the gap thickness $\dot{h}$ and the force for a fluid between circular parallel plates is derived by Dienes and Klemm[14] and presented by Bajaj et al.;[15]

$$F = -\frac{3\mu\pi r^4 \dot{h}}{2h^3}, \tag{5}$$

where F is the force, μ is the Newtonian viscosity, r is the radius of the plates and $\dot{h}$ the rate of change of distance between the plates or the gap thickness. This equation is an approximation and in the experiment, the bottom

plate is much larger than the top one. The gap thickness, $h(t)$, with time, t, can be derived from equation 5;[15]

$$h(t) = \frac{1}{\sqrt{\frac{4Ft}{3\pi\mu r^4} + \frac{1}{h_0^2}}}, \tag{6}$$

where h_0 is the initial gap thickness. The results of the experiment cannot be explained with equation 6, assuming a molten layer-thickness described by Figure 6 and a viscosity of 0.0021 Pas (assuming 327°C).[16] Table 1 shows a test case with a molten geometry based off Figure 6, and a second test case with a larger diameter and thinner molten thickness.

Parameter	Test Case 1	Test Case 2
Applied Force	2 N	
Viscosity	0.0021 Pas	
Molten Time	0.1 ms	
Plate Diameter	1 mm	2 mm
Initial Height	10 μm	1 μm
Gap-Thickness Change	8,800 nm	20 nm

Table 1: Predictions via equation 6 of gap-thickness change for different molten-layer diameters and thicknesses.

The first case predicts a gap-thickness change two orders of magnitude too high, while the second is close to the experimental data. The molten geometry is likely different than the calculations and the heating process should be further understood. It is likely that the edges of the solder joint were not melted and therefore modeling this as fluid between two plates is not valid. Furthermore it is possible the solder is not being heated enough to fully liquify and is just momentarily softening from the heat.

More precisely controlled experiments could explain the results and also answer questions about the technology. Specifically measuring the solder bond strength before and after laser irradiation would determine if the process weakens the bonds. This would require a repeatable soldering process which could be done with an oven and carefully machined bulbs of solder. It is also possible the glass is getting compressed or stretched and compressive tests could be done without solder to look for changes in gap thickness. Furthermore, experiments should be done with alternative solders containing bismuth, tin, lead, indium and cadmium that have much lower melting points (<50°C).[17]

6. CONCLUSION

Preliminary results from liquid metal actuation show that it is a promising technique to adjust glass-to-metal joints. Modeling shows that a ∼1 μm-thick layer of solder can be melted by a laser pulse ∼1 ms and 100 Watts. An experimental apparatus was built to test whether a bond between Kovar and D263 glass via Pb/Sn solder could be adjusted. The results showed that the joints could become larger with tensile force and shrink under compression with a precision $<$ 100 nm depending on the force, laser pulse time and intensity. These results are preliminary and future experiments should be done to further understand the process. Furthermore, low-temperature solders need to be evaluated for developing a bonding process that will avoid warping sensitive materials such as x-ray telescope materials.

ACKNOWLEDGMENTS

This work was supported in part by NASA grant NNX14AE76G and the MIT Kavli Institute and the NSF Graduate Research Fellowships Program (GRFP). Specific thanks to Charlie Bridge and Steven Wirta at IPG Photonics Inc. and James Daley of the MIT Nanostructures Lab.

REFERENCES

[1] O'Dell, S. L., Brissenden, R. J., Davis, W. N., Elsner, R. F., Elvis, M. S., Freeman, M. D., Gaetz, T., Gorenstein, P., Gubarev, M. V., Jerius, D., Juda, M., Kolodziejczak, J. J., Murray, S. S., Petre, R., Podgorski, W., Ramsey, B. D., Reid, P. B., Saha, T., Schwartz, D. A., Trolier-McKinstry, S., Weisskopf, M. C., Wilke, R. H. T., Wolk, S., and Zhang, W. W., "High-resolution x-ray telescopes," in [*Society of Photo-Optical Instrumentation Engineers (SPIE) Conference Series*], **7803**, 78030H (Aug. 2010).

[2] Weisskopf, M. C., Gaskin, J., Tananbaum, H., and Vikhlinin, A., "Beyond Chandra - the X-ray Surveyor," in [*Society of Photo-Optical Instrumentation Engineers (SPIE) Conference Series*], **9510**, 951002 (May 2015).

[3] Committee for a Decadal Survey of Astronomy and Astrophysics, [*New Worlds, New Horizons in Astronomy and Astrophysics*], The National Academies Press, Washington, DC (2010). `http://www.nap.edu/catalog/12951/new-worlds-new-horizons-in-astronomy-and-astrophysics`.

[4] National Aeronautics and Space Administration, "Enduring quests daring visions, NASA astrophysics in the next three decades." Website (2013). `http://science.nasa.gov/media/medialibrary/2013/12/20/secure-Astrophysics_Roadmap_2013.pdf`.

[5] Zhang, W. W., Biskach, M. P., Bly, V. T., Carter, J. M., Chan, K. W., Gaskin, J. A., Hong, M., Hohl, B. R., Jones, W. D., Kolodziejczak, J. J., Kolos, L. D., Mazzarella, J. R., McClelland, R. S., McKeon, K. P., Miller, T. M., O'Dell, S. L., Riveros, R. E., Saha, T. T., Schofield, M. J., Sharpe, M. V., and Smith, H. C., "Affordable and lightweight high-resolution x-ray optics for astronomical missions," in [*Society of Photo-Optical Instrumentation Engineers (SPIE) Conference Series*], **9144**, 914415 (July 2014).

[6] McClelland, R. S., Biskach, M. P., Chan, K.-W., Espina, R. A., Hohl, B. R., Saha, T. T., and Zhang, W. W., "Process of constructing a lightweight x-ray flight mirror assembly," in [*Society of Photo-Optical Instrumentation Engineers (SPIE) Conference Series*], **9144**, 914441 (July 2014).

[7] Broadway, D. M., Weimer, J., Gurgew, D., Lis, T., Ramsey, B. D., O'Dell, S. L., Gubarev, M., Ames, A., and Bruni, R., "Achieving zero stress in iridium, chromium, and nickel thin films," in [*Society of Photo-Optical Instrumentation Engineers (SPIE) Conference Series*], **9510**, 95100E (2015).

[8] Chalifoux, B., Heilmann, R. K., and Schattenburg, M. L., "Shaping of thin glass X-ray telescope mirrors using air bearing slumping and ion implantation," in [*Society of Photo-Optical Instrumentation Engineers (SPIE) Conference Series*], **9144**, 91444D (July 2014).

[9] Chan, K.-W., Zhang, W. W., Sharpe, M. V., Mazzarella, J. R., McClelland, R. S., Biskach, M. P., Saha, T. T., Kolos, L. D., and Hong, M.-L., "Preserving accurate figures in coating and bonding mirrors for lightweight x-ray telescopes," in [*Society of Photo-Optical Instrumentation Engineers (SPIE) Conference Series*], **9144**, 914440 (July 2014).

[10] Zhuang, J., Werner, K., and Schlünder, E.-U., "Study of the analytical solution to the heat transfer problem and surface temperature in a semi-infinite body with a constant heat flux at the surface and an initial temperature distribution," *Heat and Mass Transfer* **30**(3), 183–186 (1995).

[11] IPG Photonics Corporation, "IPG photonics' application facilities - developing your laser solution." Website (July 2015). `http://www.ipgphotonics.com/application_facilities_worldwide.htm`.

[12] Beardmore, R., "Loaded flat plates." Website (July 2015). `http://www.roymech.co.uk/Useful_Tables/Mechanics/Plates.html`.

[13] Präzisions Glas & Optik, "D263 T borosilicate thin glass." Website (July 2015). `http://www.pgo-online.com/intl/katalog/D263.html`.

[14] Dienes, G. J. and Klemm, H. F., "Theory and application of the parallel plate plastometer," *Journal of Applied Physics* **17**(6) (1946).

[15] Bajaj, N., Subbarayan, G., and Garimella, S. V., "Topological design of channels for squeeze flow optimization of thermal interface materials," *International Journal of Heat and Mass Transfer* **55**(1314), 3560 – 3575 (2012).

[16] CINDAS, "Report 102," (1991).

[17] Indium Corporation, "Low temperature alloys." Website (July 2015). `http://www.indium.com/low-temperature-alloys/`.